International Journal of Pharmacy and Pharmaceutical Sciences

ISSN- 0975-1491 Vol 3, Suppl 1, 2011

Full Proceeding Paper

SOLID PHASE MICROBIAL TRANSFORMATION OF CORTEXOLONE AND PROLYL ENDOPEPTIDASE INHIBIOTORY ACTIVITY OF THE TRANSFORMED PRODUCTS

*,1 SYED ADNAN ALI SHAH, 1SADIA SULTAN, 2HUMERA SYED ADNAN

*,1Institut Kajian Ubat Semulajadi (iKUS), Faculty of Pharmacy, Universiti Teknologi MARA (UiTM), Campus Puncak Alam, 42300 Puncak Alam, Selangor D. E, Malaysia. 2H. E. J. Research Institute of Chemistry, International Center for Chemical and Biological Sciences, University of Karachi, Karachi 75270, Pakistan. Email: syedadnan@salam.uitm.edu.my, benzene301@yahoo.com

ABSTRACT

Structural transformation of cortexolone (**1**) was carried out by fungi, *Rhizophus stolonifer* (TSY 0471), *Fusarium lini* (NRRL 68751) and *Cunninghamella elegans* (TSY 0865) using solid phase technology, resulted in the formation of ten polar metabolites. These metabolites were identified as 17α,21-dihydroxypregn-1,4-dien-3,20-dione (**2**), 16β,17α,21-trihydroxypregn-1,4-dien-3,20-dione (**3**), 17α,21-dihydroxypregn-1,4-dien-3,11,20-trione (**4**), 15β,17α,21-trihydroxypregn-4-en-3,20-dione (**5**), androsta-1,4-diene-3,17-dione (**6**), 17β-hydroxyandrosta-1,4-dien-3-one (**7**), 16β,17β-dihydroxyandrosta-1,4-dien-3-one (**8**), 11α,17β-dihydroxyandrosta-1,4-dien-3-one (**9**), 16β-hydroxyandrosta-1,4-dien-3,17-dione (**10**), and 15β-hydroxyandrosta-1,4-diene-3-one (**11**). Metabolite **10** was found to be new. Metabolite **3** and **9** have exhibited good activity against the prolyl endopeptidase enzyme.

Keywords: Cortexolone, Microbial transformation, Solid phase technology and Prolyl endopeptidase.

INTRODUCTION

Cortexolone (Reichstein compound S) (**1**) is a glucocorticoid receptor antagonist, used for the treatment of dementia[1]. Microorganisms are capable of converting a whole range of organic compounds into their modified derivatives[2-10]. Microbial transformations have been extensively applied in the productions of several therapeutically important steroids on commercial scale. Such studies are primarily useful in the generation of hydoxylated metabolites for drug toxicity studies[2-10]. In continuation of work on microbial transformation of various bioactive compounds[2-10,19], cortexolone (**1**) was incubated with three different fungi strains by using solid phase technology[11]. Structures of transformed products were deduced through the spectroscopic techniques and prolyl endopeptidase inhibitory effect was monitored. Prolyl endopeptidase (PEP, EC 3.4.21.26), which is a member of a new class of serine peptidases, catalyzes the cleavage peptide of bond at the carboxyl side of proline residue and is involved in the biological regulation of proline-containing neuropeptides and peptide hormones, which are known to be involved in learning and memory[12-14]. All these efforts have been recently made to search for new PEP inhibitors leading to the development of anti-dementia drugs.

EXPERIMENTAL

Instrumentation

The ^{1}H-NMR spectra (δ ppm, *J* in Hz) were recorded in deuterated solvent ($CDCl_3$) at 400 MHz and 500 MHz on Bruker Avance-400 and Avance-500 NMR spectrometers, while ^{13}C-NMR spectra were recorded in $CDCl_3$ on same instruments at 100 MHz and 125 MHz, respectively. A Varian MAT 311A mass spectrometer, connected to a Mass Data system was used to record the mass spectra. The HRMS(EI) spectra were recorded on Jeol JMS-600H mass spectrometer. The FT-IR was recorded on Shimadzu FTIR-8900 spectrophotometer and UV spectra were recorded on Advance UV spectrophotometer. Optical rotation measurements were performed on a Jasco DIP 360 digital polarimeter. Melting points were taken on a Buchi 535 apparatus. The purity of the samples was checked on precoated plates (Si gel 60, F_{254} 0.2 mm, E. Merck). The metabolites were purified by flash column and on precoated TLC plates (Si gel 60, F_{254} 0.2 mm, E. Merck).

Fermentation of Cortexolone by *Rhizopus stolonifer* (TSY 0471), *Fusarium lini* (NRRL 68751) and *Cunninghamella elegans* (TSY 0865)

Media for each fungus was prepared by adding Sabouraud-4% glucose-agar (Merck) (120 g) in 3 L. The solution was boiled on a hot plate and then poured in 100 mL flasks and autoclaved at 123° C. The fungi was inoculated on the solid phase media and allowed to grow for two days at 28° C. The cortexolone (**1**) (1 g) was dissolved in acetone (15 mL) and fed in each flask (0.5 mL) and subsequently kept for 4 days. The positive control contained only the substrate **1** while negative control contained only fungal growth. After 4 days, all flasks were extracted using dichloromethane to obtain a crude extract (amounting of 1.45 g). Six metabolites **2-7** were obtained from *Rhizopus stolonifer* media, three transformed products **5-7** were observed from *Fusarium lini* and six metabolites **8-12** were obtained from *Cunninghamella elegans* by using column chromatography (Fig. 1).

17α,21-Dihydroxypregn-1,4-dien-3,20-dione (2)

Colorless crystalline solid; Yield 20%; mp 180-183°C; $[\alpha]_D^{25}$: – 56 (EtOH, *c* = 0.4); UV ($CHCl_3$) λ_{max} (log ε): 243 (3.2) nm; IR ν_{max} cm^{-1} ($CHCl_3$): 3394 (OH), 1712 (CO, ketonic) and 1656 (C=C); ^{1}H NMR ($CDCl_3$) spectral data (Table 1). ^{13}C NMR ($CDCl_3$) spectral data (Table 3). EI MS *m/z* (rel. int., %): 344 (4) [M$^+$], 285 (13), 159 (15), 147 (58), 121 (100), 91 (37), 55 (34); HRMS(EI) (*m/z*): 344.1254 [M$^+$] (calcd for $C_{21}H_{28}O_4$, 344.1264).

16β,17α,21-Trihydroxypregn-1,4-dien-3,20-dione (3)

Colorless crystalline solid; Yield 12%; mp 184-185°C; $[\alpha]_D^{25}$: – 41 (EtOH, *c* = 0.4); UV ($CHCl_3$) λ_{max} (log ε): 244 (3.4) nm; IR ν_{max} cm^{-1} ($CHCl_3$): 3384 (OH), 1715 (CO, ketonic) and 1648 (C=C); ^{1}H NMR ($CDCl_3$) spectral data (Table 1). ^{13}C NMR ($CDCl_3$) spectral data (Table 3). EI MS: *m/z* (rel. int.,%): 359.8 (3) [M$^+$], 302 (20), 300 (14), 289 (25), 271 (26), 244 (15), 213 (9), 122 (99), 91 (47), 55 (100); HRMS(EI) (*m/z*): 360.2457 [M$^+$] (calcd for $C_{21}H_{28}O_5$, 360.2468).

17α,21-Dihydroxypregn-1,4-dien-3,11,20-trione (4)

Colorless crystalline solid; Yield 34%; mp 155°C; $[\alpha]_D^{25}$: +109 (EtOH, *c* = 4.0); UV ($CHCl_3$) λ_{max} (log ε): 242.5 (2.1) nm; IR ν_{max} cm^{-1} ($CHCl_3$): IR ($CHCl_3$) ν_{max}: 3448 (OH), 1737 (CO, ketonic) and 1662 (C=C); ^{1}H NMR ($CDCl_3$) spectral data (Table 1). ^{13}C NMR ($CDCl_3$) spectral data (Table 3). EI-MS *m/z* (rel. int., %): 358 (70) [M$^+$], 302 (21), 289 (17), 91 (99), 55 (100); HRMS(EI) (*m/z*): 358.1528 [M$^+$] (calcd for $C_{21}H_{26}O_5$, 358.1536).

15β,17α,21-Trihydroxypregn-4-en-3,20-dione (5)

Colorless crystalline solid; Yield 20%; mp 271-273°C; $[\propto]_D^{25}$: – 48 (MeOH, *c* = 0.16); UV ($CHCl_3$) λ_{max} (log ε): 242 (2.4) nm; IR ν_{max} cm^{-1} ($CHCl_3$): IR ($CHCl_3$) ν_{max}: 3475 (OH), 1727 (CO, ketonic) and 1656 (C=C); ^{1}H NMR ($CDCl_3$) spectral data (Table 1). ^{13}C NMR ($CDCl_3$) spectral data (Table 3). EI-MS *m/z* (rel. int., %): 362 (26) [M$^+$], 344 (21), 302 (26), 285 (60), 163 (55), 123 (62), 91 (50), 55 (100); HRMS(EI) (*m/z*): 362.2675 [M$^+$] (calcd for $C_{21}H_{30}O_5$, 362.2786).

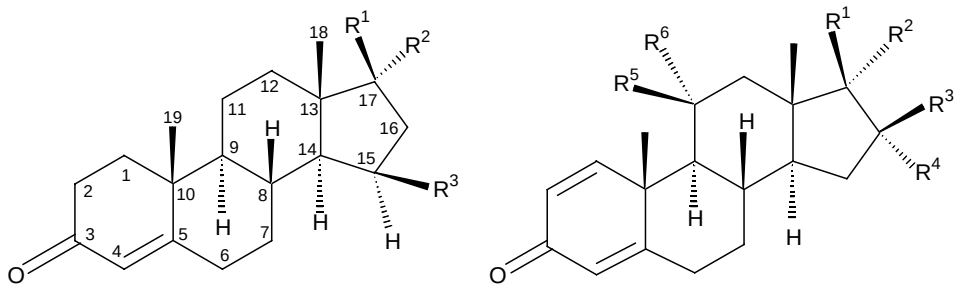

1 $R^1 = -\underset{20}{C}(=O)-\underset{21}{CH_2OH}$, $R^2 = OH$, $R^3 = H$

5 $R^1 = -\underset{20}{C}(=O)-\underset{21}{CH_2OH}$, $R^2 = R^3 = OH$

11 $R^1 = R^2 = O$, $R^3 = OH$

2 $R^1 = -\underset{20}{C}(=O)-\underset{21}{CH_2OH}$, $R^2 = OH$
$R^3 = R^4 = R^5 = R^6 = H$

3 $R^1 = -\underset{20}{C}(=O)-\underset{21}{CH_2OH}$, $R^2 = R^3 = OH$
$R^4 = R^5 = R^6 = H$

4 $R^1 = -\underset{20}{C}(=O)-\underset{21}{CH_2OH}$, $R^2 = OH$
$R^3 = R^4 = H$, $R^5 = R^6 = O$

6 $R^1 = R^2 = O$, $R^3 = R^4 = R^5 = R^6 = H$

7 $R^1 = OH$, $R^2 = R^3 = R^4 = R^5 = R^6 = H$

8 $R^1 = R^3 = OH$, $R^2 = R^4 = R^5 = R^6 = H$

9 $R^1 = R^6 = OH$, $R^2 = R^3 = R^4 = R^5 = H$

10 $R^1 = R^2 = O$, $R^3 = OH$, $R^4 = R^5 = R^6 = H$

Fig. 1: Products of solid phase fermentation of cortexolone (1) with *Rhizopus stolonifer, Fusarium lini* and *Cunninghamella elegans*

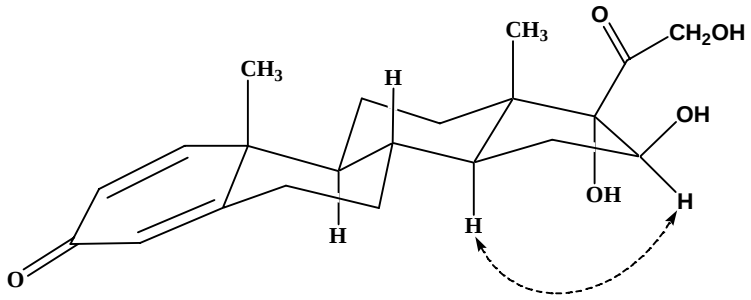

Fig. 2: Key correlations of compound 3 in NOESY spectrum

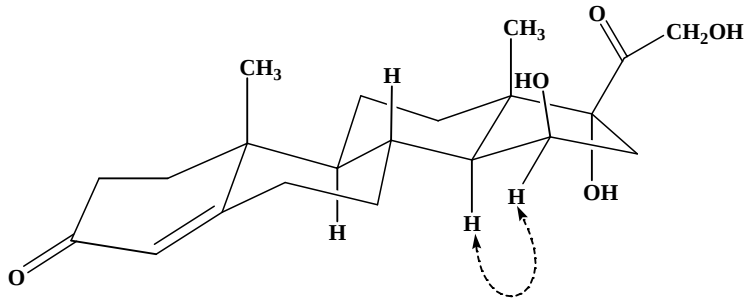

Fig. 3: Key correlations of compound 5 in NOESY spectrum

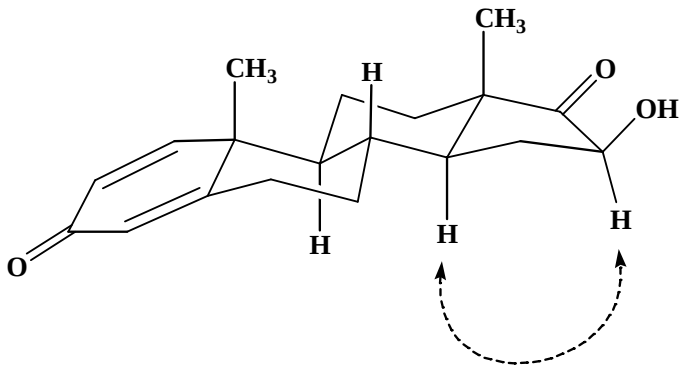

Fig. 4: Key correlations of compound 10 in NOESY spectrum

Androsta-1,4-diene-3,17-dione (6)

Colorless solid; Yield 11%; mp 221-224°C; $[\propto]_D^{25}$:– 61 (MeOH, *c* = 0.1); UV ($CHCl_3$) λ_{max} (log ε): 258 (3.8) nm; IR ν_{max} cm^{-1} ($CHCl_3$): IR ($CHCl_3$) ν_{max}: 1726 (CO, ketonic) and 1643 (C=C); ^1H NMR ($CDCl_3$) spectral data (Table 1). ^{13}C NMR ($CDCl_3$) spectral data (Table 3). EI-MS *m/z* (rel. int., %): 284 (62) [M^+], 227 (13), 194 (14), 181 (53), 135 (50), 122 (100), 91 (60), 55 (91); HRMS(EI): (*m/z*) 284.1428 [M^+] (calcd for $C_{19}H_{24}O_2$, 284.1344).

17β-Hydroxyandrosta-1,4-dien-3-one (7)

Colorless solid; Yield 12%; mp 212-214°C; $[\propto]_D^{25}$:– 161 (MeOH, *c* = 0.1); UV ($CHCl_3$) λ_{max} (log ε): 248 (3.4) nm; IR ν_{max} cm^{-1} ($CHCl_3$): 3339 (OH), 1727 (CO, ketonic) and 1653 (C=C); ^1H NMR ($CDCl_3$) spectral data (Table 2). ^{13}C NMR ($CDCl_3$) spectral data (Table 3). EI-MS *m/z* (rel. int., %): 286 (48) [M^+], 284 (26), 181 (53), 135 (50), 122 (100), 91 (60), 55 (90); HRMS(EI): (*m/z*) 286.1246 [M^+] (calcd for $C_{19}H_{26}O_2$, 286.1311).

16β,17β-Dihydroxyandrosta-1,4-dien-3-one (8)

Colorless solid; Yield 10%; mp 221-223°C; $[\propto]_D^{25}$: – 121 (MeOH; *c* = 0.1); UV ($CHCl_3$) λ_{max} (log ε): 255 (4.4) nm; IR ν_{max} cm^{-1} ($CHCl_3$): 3328 (OH), 1717 (CO, ketonic), 1651 (C=C); ^1H NMR ($CDCl_3$) spectral data (Table 2). ^{13}C NMR ($CDCl_3$) spectral data (Table 3). EI-MS *m/z* (rel. int., %): 302 (4) [M^+], 193 (12), 149 (100), 104 (11), 59 (21), 91 (89), 55 (20); HRMS(EI): (*m/z*) 302.2415 [M^+] (calcd for $C_{19}H_{26}O_3$, 302.2516).

11α,17β-Dihydroxyandrosta-1,4-dien-3-one (9)

Colorless solid; Yield 15%; mp 217-220°C; $[\propto]_D^{25}$: – 61 (MeOH, *c* = 0.1); UV ($CHCl_3$) λ_{max} (log ε): 258.2 (3.4) nm; IR ν_{max} cm^{-1} ($CHCl_3$): 3325 (OH), 1737 (CO, ketonic), 1661 (C=C); ^1H NMR ($CDCl_3$) spectral data (Table 2). ^{13}C NMR ($CDCl_3$) spectral data (Table 3). EI-MS *m/z* (rel. int., %): 302 (48) [M^+], 284 (26), 181 (53), 135 (50), 122 (100), 91 (60), 55 (90); HRMS(EI): (*m/z*) 302.1354 [M^+] (calcd for $C_{19}H_{26}O_3$, 302.1453).

16β-Hydroxyandrosta-1,4-dien-3,17-dione (10)

Colorless solid; Yield 15%; mp 207-210°C; $[\propto]_D^{25}$: – 124 (*c* = 0.1, MeOH); UV ($CHCl_3$) λ_{max} (log ε): 244 (4.3) nm; IR ν_{max} cm^{-1} ($CHCl_3$): 3320 (OH), 1735 (CO, ketonic), 1657 (C=C) cm^{-1}; ^1H NMR ($CDCl_3$) spectral data (Table 2). ^{13}C NMR ($CDCl_3$) spectral data (Table 3). EI-MS *m/z* (rel. int., %): 300 (6) [M^+], 284 (50), 181 (35), 149 (18), 91 (90), 55 (100); HRMS(EI): (*m/z*) 300.2367 [M^+] (calcd for $C_{19}H_{24}O_3$, 300.2378).

15β-Hydroxyandrosta-1,4-diene-3-one (11)

Colorless solid; Yield 15%; mp 202-204°C; $[\propto]_D^{25}$: – 87 (*c* = 0.1, MeOH); UV ($CHCl_3$) λ_{max} (log ε): 242 (3.8) nm; IR ν_{max} cm^{-1} ($CHCl_3$): 3328 (OH), 1725 (CO, ketonic), 1667 (C=C); ^1H NMR ($CDCl_3$) spectral data (Table 2). ^{13}C NMR ($CDCl_3$) spectral data (Table 3). EI-MS *m/z* (rel.int., %): 300 (6) [M^+], 284 (50), 181 (35) , 149 (18), 91 (90), 55 (100); HRMS(EI): (*m/z*) 300.2244 (calcd for $C_{19}H_{24}O_3$, 300.2244).

Table 1: ^1H NMR (400 MHz) Data of Compounds 2-6 (δ, $CDCl_3$)

Position of proton	Cpd 2	Cpd 3	Cpd 4	Cpd 5	Cpd 6
1	7.02 (d, 10.1)	7.03 (d, 10.2)	7.61 (d, 10.2)	2.36 (m)	7.02 (d, 10.1)
2	6.21 (dd, 10.1, 1.8)	6.20 (dd, 10.1, 1.7)	6.10 (dd, 10.2, 1.8)	2.24 (m)	6.22 (dd, 10.1, 1.7)
3	-	-	-	-	-
4	6.05 (s)	6.02 (s)	6.01 (s)	5.71 (s)	6.08 (s)
5	-	-	-	-	-
6	2.10 (m)	2.10 (m)	2.11 (m)	2.14 (m)	2.12 (m)
7	2.31 (m)	2.30 (m)	2.32 (m)	1.91 (m)	2. 23 (m)
8	1.41 (m)	1.42 (m)	1.41 (m)	1.42 (m)	1.41 (m)
9	1.44 (m)	1.44 (m)	1.84 (m)	1.45 (m)	1.42 (m)
10	-	-	-	-	-
11	1.84 (m)	1.82 (m)	-	1.88 (m)	1.81 (m)
12	1.73 (m)	1.69 (m)	1.92 (m)	1.70 (m)	1.72 (m)
13	-	-	-	-	-
14	1.57 m	1.57 (m)	1.54 (m)	1.75 m	1.53 (m)
15	1.62 (m)	2.13 (m)	2.12 (m)	3.98 (m, $W_{1/2}$ = 14.0)	2.14 (m)
16	2.25 (m)	3.62 (d, 3.1)	2.22 (m)	2.28 (m)	2.24 (m)
17	-	-	-	-	-
18	0.84 (s)	0.82 (s)	0.84(s)	0.90 s	0.81(s)
19	0.99 (s)	1.01 (s)	1.02 (s)	1.04 (s)	0.98 (s)
20	-	-	-	-	-
21	4.30 (d, 20.0), 4.64 (d, 19.9)	4.29 (d, 20.2), 4.64 (d, 19.8)	4.32 (d, 20.1), 4.62 (d, 20.0)	4.30 (d, 20.2), 4.60 (d, 20.4)	-

Table 2: ^{1}H NMR (400 MHz) Data of Compounds 7-11 (δ, $CDCl_3$)

Position of proton	Cpd 7	Cpd 8	Cpd 9	Cpd 10	Cpd 11
1	7.02 (d, 10.1)	7.01 (d, 10.3)	7.73 (d, 10.3)	7.05 (d, 10.3)	7.04 (d, 10.1)
2	6.22 (dd, 10.0, 1.7)	6.24 (dd, 10.1, 1.9)	6.22 (dd, 10.1, 1.7)	6.21 (dd, 9.9, 1.6)	6.21 (dd, 10.2, 1.8)
3	-	-	-	-	-
4	6.02 (s)	6.01 (s)	6.02 (s)	6.05 (s)	6.01 (s)
5	-	-	-	-	-
6	2.11 (m)	2.12 (m)	2.10 (m)	2.13 (m)	2.12 (m)
7	2. 23 (m)	2. 21 (m)	2. 21 (m)	2. 20 (m)	2. 23 (m)
8	1.42 (m)	1.40 (m)	1.39 (m)	1.41 (m)	1.40 (m)
9	1.44 (m)	1.44 (m)	1.84 (m)	1.46 (m)	1.42 (m)
10	-	-	-	-	-
11	1.80 (m)	1.81 (m)	4.08 (m)	1.79 (m)	1.77 (m)
12	1.72 (m)	1.73 (m)	1.90 (m)	1.75 (m)	1.72 (m)
13	-	-	-	-	-
14	1.52 (m)	1.50 (m)	1.45 (m)	1.33 (m)	1.75 (m)
15	2.10 (m)	2.15 (m)	2.11 (m)	2.16 (m)	4.30 (dd, 15.9, 7.9)
16	2.14 (m)	4.56 (ddd, 9.7, 7.4, 2.1)	2.18 (m)	3.72 (t, 5.1)	2.12 (m)
17	3.93 (t, 8.6)	3.94 (t, 7.76)	3.93 (t, 7.67)	-	-
18	0.84(s)	0.85(s)	0.82 (s)	0.83 (s)	0.87 (s)
19	0.99 (s)	1.02 (s)	1.01 (s)	1.02 (s)	0.98 (s)

Table 3: ^{13}C NMR (100 and 125 MHz) Data of Compounds 2-11 (δ, $CDCl_3$)

Position of carbon	Cpd 2	Cpd 3	Cpd 4	Cpd 5	Cpd 6	Cpd 7	Cpd 8	Cpd 9	Cpd 10	Cpd 11
1	155	155.2	154.7	25.6	155	155	155	155.4	155	155.4
2	126.5	126.5	126.3	38.3	126	126	126	127.1	126.2	127.1
3	202	201	202	198	199	199	201	201	202	203
4	124.4	125.1	124.2	124.4	124	124.4	124.4	124.3	124.5	124.3
5	148.2	148.3	148.2	164.1	148.1	148.5	148.3	148.5	148.3	148.5
6	31.6	31.6	31.6	31.4	31.3	31.3	31.3	31.3	31.3	31.3
7	30.8	30.5	30.8	29.9	30.3	30.3	30.4	30.3	30.4	30.3
8	51.3	51.3	51.6	38.1	51.6	51.4	51.6	51.4	51.6	51.4
9	54.2	54.2	52.2	58.2	52.2	52.2	52.2	60.3	52.2	60.3
10	45.2	45.3	45.1	38.7	45.1	45.1	45.1	45.1	45.1	45.1
11	21.2	21.2	199	22.1	21.8	21.6	21.8	66.8	21.8	66.8
12	39.3	39.4	42.3	34.5	37.3	37.3	37.3	39.2	37.3	39.2
13	44.9	44.9	44.9	42.4	44.9	44.5	44.9	44.5	44.9	44.5
14	50.1	50.1	50.1	49.8	50.4	50.4	50.4	50.3	50.4	50.3
15	25.2	28.2	25.2	68.5	25.2	25.2	27.2	25.1	27.2	68.5
16	22.6	67.5	22.6	34.3	27.6	27.4	75.1	26.9	74.5	26.9
17	79	79.5	79.1	215.1	217	81.7	81.7	81.7	215	216
18	13.7	14.1	14.1	13.4	14.3	13.9	14.2	13.8	14.4	13.8
19	17.3	18.3	17.2	18.1	18.2	18.1	18.7	18.2	18.3	18.2
20	216	215.2	215.6	215.2	-	-	-	-	-	-
21	62.5	62.3	62.4	62.3	-	-	-	-	-	-

PEP Inhibitory Assay

Prolyl endopeptidase (*Flavobacterium meningosepticum* origin) was purchased from Seikagaku Corporation (Tokyo, Japan). Bacitracin was purchased from Sigma Co., Ltd. and *N*-benzyloxycarbonyl-Gly-Pro-*p*NA was procured from Bachem Fine Chemicals Co. PEP inhibitory assay was performed according to previous literature[14].

RESULTS AND DISCUSSION

Compound 1 ($C_{21}H_{30}O_4$) was incubated in solid media with *Rhizopus stolonifer* and *Fusarium lini* for 4 days. Known metabolites 2-7 were obtained from *Rhizopus stolonifer*, while metabolites 5-7 were isolated from *Fusarium lini* by column chromatographic techniques and structures of the metabolites were identified by spectroscopic analysis (Fig. 1). The HRMS(EI) of compound 2 exhibited the M^+ at *m/z* 344.1254 ($C_{21}H_{28}O_4$, calcd 344.1264). The IR spectrum showed absorptions for hydroxyl, carbonyl and olefinic functionalities at 3394, 1712 and 1656 cm^{-1}, respectively. The UV spectrum exhibited the presence of chromophore at 243 nm. The ^{1}H-NMR spectrum of compound 2 displayed two additional downfield olefinic proton signals at δ 7.02 (d, $J_{1,2}$ = 10.1 Hz, H-1) and 6.21 (dd, $J_{2.1}$ = 10.1 Hz, $J_{2.4}$ = 1.8 Hz, H-2). The COSY-45° spectrum showed couplings between H-1 (δ 7.02) and H-2 (δ 6.21) indicating the presence of a double bond between C-1/C-2. The ^{13}C-NMR spectrum showed two additional olefinic carbon signals at δ 155.0 (C-1) and 127.0 (C-2). The HMBC couplings between C-3 (δ 199) and H-1 (δ 7.02), H-2 (δ 6.21) and H-4 (δ 6.02), further supported an unsaturation between C-1/C-2.

The above described spectral data and comparison with literature values led us to concluded that metabolite 2 is 17α,21-dihydroxy-pregn-1,4-dien-3,20-dione[16].The hydroxylated derivative **3** showed the M^+ at *m/z* 360.2457 ($C_{21}H_{28}O_5$, calcd 360.2468). The peak at *m/z* 342 arose due to the loss of a water molecule. The presence of a hydroxyl moiety was further inferred from the ^{1}H-NMR spectrum, which showed a doublet at δ 3.62 (1H, $J_{16\alpha 15\beta}$ = 3.1 Hz, H-16α).

The IR and UV of compound **3** were distinctly similar to compound **2**. The DEPT experiment showed an additional signal of a hydroxylated methine carbon at δ 67.5, assigned to C-16 based on its HMBC coupling with H_2-15 (δ 2.1, 1.45). The β-orientation of newly introduced hydroxyl at C-16 was inferred from the NOESY cross

peak between H-16 (δ 3.62) and H-14 (δ 1.4) (Fig. 2). The above spectral data and comparison with literature values showed that **3** is 16β,17α,21-trihydroxy-pregn-1,4-dien-3,20-dione[16].

Metabolite **4** showed the M+ at *m/z* 358.1528 ($C_{21}H_{26}O_5$, calcd 358.1536, HRMS). The UV and IR absorptions of compound **4** were found to be similar to compound **2**, but ^{1}H-NMR spectrum exhibited a deshielded signal at δ 7.61 (1H, d, $J_{1,2}$ = 10.2 Hz, H-1) due to an anisotropic effect of C-11 carbonyl group. A new quaternary carbon signal at δ 201.0 in Broad-band (decoupled) spectrum was assigned to C-11 on the basis of HMBC correlations of H-9 (δ 1.70) with C-11 (δ 201.0), while H-1 (δ 7.61) showed ^2J heteronuclear coupling with C-2 (δ 127.0) indicating an unsaturation site between C-1/C-2. From the above mentioned spectral data and comparison with literature values[16], the structure for metabolite **4** was deduced as 17α,21-dihydroxypregn-1,4-dien-3,11,20-trione

Table 4: Inhibitory Activity [IC_{50} (μM)] of Compounds for Prolyl Endopeptidase (PEP)

Compound	*IC_{50} (μM)
1	8.17± 0.22
2	22.63± 1.58
3	8.62± 0.55
5	31.11± 1.47
8	48.61± 2.15
9	16.55± 1.52
Bacitracin (Positive control)	129.26 ± 3.28

*IC_{50} values are the mean ± standard error mean (SEM) of three assays.

Metabolites **4, 6**, **7**, **10** and **11** were not tested due to insufficient quantity.

The hydroxyl-bearing metabolite **5** showed the M+ at *m/z* 362.2675 ($C_{21}H_{30}O_5$, calcd 362.2786) in HRMS(EI). The UV spectrum displayed absorption at 242 nm. The ^{1}H-NMR spectrum exhibited an additional methine proton signal at δ 3.98 (m, $W_{1/2}$ = 14.0 Hz, H-15α) which was coupled with H_2-16 (δ 2.28) and H-14 (δ 1.75), indicating an OH group at C-15 position. The DEPT spectrum possesses a downfield methine signal at δ 68.5, assigned to C-15 based on the HMBC couplings of C-15 with H_2-16 and H-14. The β-stereochemistry of 15-OH was inferred from NOESY experiment which showed dipolar coupling between H-15α (δ 3.98) and H-14 (δ 1.75) (Fig. 3). The structure of metabolite **5** thus was identified as 15β,17α,21-trihydroxypregn-4-en-3,20-dione.

Compound **1** was also fermented on solid phase *Cunninghamella elegans*, for 7 days to obtain bio-degradative metabolites **6-11** (Fig. 1). The HRMS(EI) of compound **6** showed the M+ at *m/z* 284.1428 ($C_{19}H_{24}O_2$, calcd 284.1344). The IR spectrum showed absorption bands for ketonic and olefinic functionalities at 1726 and 1653 cm^{-1}, respectively. The UV spectrum showed strong absorption at 243 nm. The ^{1}H-NMR spectrum displayed two olefinic proton signals at δ 7.02 (d, $J_{1,2}$ = 10.1 Hz, H-1), and 6.22 (dd, $J_{2,1}$ = 10.1 Hz, $J_{2,4}$ = 1.7 Hz, H-2), and a singlet for H-4 at δ 6.08. The absence of an AB doublets, as compared to substrate **1**, indicated the oxidative cleavage of C-17 side chain. The COSY- 45° spectrum showed correlations between H-1 and H-2, and H-2 and H-4, which indicated unsaturation between C-1 and C-2. The HMBC, HMQC and other spectral data further supported the structure **6** as androsta-1,4-diene-3,17-dione.

Compound **7**, a reductive product of compound **6**, showed the molecular ion at *m/z* 286.1246 in agreement of formula $C_{19}H_{26}O_2$ (calcd 286.1311). The IR spectrum showed absorption at 3339 cm^{-1} for free hydroxyl group, while the UV spectrum showed a similarity with compound **6.** The ^{1}H-NMR spectrum displayed a triplet at δ 3.93 (1H, $J_{17,16}$ = 8.6 Hz) assigned to C-17α proton. The COSY-45° displayed couplings between H-17 (δ 3.93) and H_2-16 (δ 2.1, 1.67), which indicated a regioselective reduction of C-17 ketonic carbonyl function. The HMBC spectrum showed correlations of H_2-16 (δ 2.1, 1.67) with C-17 (δ 81.7). The β-orientation of C-17 hydroxyl was deduced on the basis of coupling constant ($J_{17\alpha,16}$ = 8.6 Hz) of geminal C-17 proton with C-16 proton. The above spectral data and comparison with literature values led to the structure of metabolite **7** as 17β-hydroxyandrosta-1,4-dien-3-one[17].

The compound **8** was identified as hydroxylated metabolite of compound **7** with the M+ at *m/z* 302.2415 having a formula $C_{19}H_{26}O_3$ (calcd 302.2516) through HRMS(EI). The ^{1}H-NMR displayed a doublet of double doublet at δ 4.56 (1H, $J_{16\alpha,15\beta}$ = 2.1 Hz, $J_{16\alpha,17\alpha}$ = 7.4 Hz, $J_{16\alpha,15\alpha}$ = 9.7 Hz, H-16α) and a doublet at δ 3.94 (1H, $J_{17,16\alpha}$ = 7.7 Hz, H-17α). The COSY 45° spectrum exhibited coupling between H-17α (δ 3.94) and H-16α (δ 4.56). The DEPT spectrum showed an additional methine carbon signal at δ 75.1 (C-16), as compared to compound **7**. The presence of an OH at C-16 was further inferred from the HMBC correlation between H-16 (δ 4.56) and C-17 (δ 81.7). The β-stereochemistry of OH-16 was deduced on the basis of coupling constant and NOESY correlation of H-16α (δ 4.56) with H-17α (δ 3.94). From the above mentioned spectral data and comparison with literature values[17], the structure of metabolite **8** was concluded as 16β,17β-dihydroxyandrosta-1,4-dien-3-one.

The HREI MS of compound **9** displayed the M+ at *m/z* 302.1354 ($C_{19}H_{26}O_3$, calcd 302.1453). The ^{1}H-NMR spectrum displayed a downfield olefinic proton signal at δ 7.73 (d, $J_{1,2}$ = 10.3 Hz, H-1) along with a multiplet at δ 4.08 (H-11). The position of newly introduced hydroxyl at C-11 was further deduced from the HMBC correlations of H-11 (δ 4.08) with C-9 (56.5) and COSY-45° couplings between H-11 (δ 4.08) and H_2-12 (δ 2.1, δ 1.63) and H-9α (δ 1.73). The α-stereochemistry of OH-11 was inferred from $W_{1/2}$ = 14 Hz of H-11 signal, as well as NOESY correlations between H-11β (δ 4.08), Me-18 (δ 0.82) and Me-19 (δ 1.30). From the above mentioned spectral data and comparison with literature values[15,18], the structure of metabolite **9** was concluded as 11α,17β-dihydroxyandrosta-1,4-dien-3-one.

Compound **10** was identified as a C-11 hydroxylated metabolite of compound **6,** which showed the M+ at *m/z* 300.2367 ($C_{19}H_{24}O_3$, calcd 300.2378). The IR spectrum showed the presence of a hydroxyl group (3453 cm^{-1}). The ^{1}H-NMR spectrum exhibited a triplet at δ 3.70 (1H, $J_{16\alpha,15\beta}$ = 5.1 Hz, H-16α). The position of OH at C-16 was further inferred from ^2J heteronuclear correlation of H-16 (δ 3.70) with C-17 (δ 201.0), while the COSY-45° spectrum displayed couplings of H-16 (δ 3.7) with H_2-15 (δ 1.54, 1.56) further indicating a hydroxylation at C-16 position. The β-stereochemistry of OH-16 was deduced from the NOESY correlation between H-16α (δ 3.7) and H-14α (δ 1.45) (Fig. 4). According to these spectroscopic data the structure of metabolite **10** was found to be new because of a stereochemistry of 16-OH moiety and deduced as 16β-hydroxyandrosta-1,4-dien-3,17-dione.

The compound **11** was identified as an oxidative metabolite of compound **6** with the M+ at *m/z* 300.2248 ($C_{19}H_{24}O_3$, calcd 300.2267) in HRMS(EI). The ^{1}H-NMR spectrum exhibited a double doublet at δ 4.30 (1H, *J* = 15.9 Hz, *J* = 7.9 Hz, H-15α). The position was further proved from COSY-45° spectrum which showed couplings between H-15 (δ 4.3) and H_2-16 (δ 2.1, 1.6), along with the HMBC correlations between H_2-16 (δ 2.1, 1.6) and C-15 (δ 71.5). The β-stereochemistry of newly introduced C-15 hydroxyl was deduced from the NOESY correlation between H-15α (δ 3.7) and H-14α (δ 1.75). From the

above mentioned spectral data and comparison with literature values[15], the structure of metabolite **11** was concluded as 15β-Hydroxyandrosta-1,4-diene-3-one.

The cortexolone (**1**) and their metabolites have exhibited pronounced inhibitory activity against the prolyl endopeptidase (PEP) enzyme (Table 4). The IC_{50} values of compounds are shown in Table 4 along with the positive control of PEP (Bacitracin). Some hydroxy metabolites of cortexolone (**1**) showed significant inhibitory activity against PEP enzyme, the OH at C-11, C-15, C-16 and C-17 as in metabolites **3, 5** and **9**, respectively showed pronounced inhibitory activity the against enzyme, while α, β–unsaturated system (C-1/C-2) in metabolite **2** also showed a good activity (Table 4). The hydroxyl group at C-16 (β-OH in metabolite **3**) and C-11 (α-OH in metabolite **9**) showed potent PEP inhibitory activity. While in metabolite **2**, α, β–unsaturated systems (C-1/C-2) and hydroxyl bearing moiety at C-17 showed significant activity.

CONCLUSIONS

In conclusion, the fungal transformation of cortexolone (**1**) by *Rhizophus stolonifer, Fusarium lini* and *Cunninghamella elegans* using solid phase technology yielded ten polar metabolites **2**-**11**. Metabolite **10** was found to be new. The main hydroxylations occurred in rings C and D, especially at C-11, C-15 and C-16 positions. The metabolites **2**, **3**, **5**, **8** and **9** were identified as the main metabolites of the fermentations. Metabolites **3**, **5**, and **9** containing an OH-group at C-11, C-15, C-16 and C-17, showed pronounced inhibitory activity against prolyl endopeptidase (PEP) enzyme (Table 4), while α, β–unsaturated system (C-1/C-2) in metabolite **2** also showed a good inhibitory activity (Table 4)

ACKNOWLEDGMENTS

The authors acknowledges to the Ministry of Science**,** Technology and Innovation. MOSTI, eScienceFund, Malaysia, for providing us research grant.

REFERENCES

1. Fulop V, Szeltner Z, Polgar, L. Catalysis of serine oligopeptidases is controlled by a gating filter mechanism. EMBO Reports. 2000; 1: 277-281.
2. Choudhary MI, Shah SAA, Atta-ur-Rahman. Microbial Oxidation of Anabolic Steroids. Nat Prod Res. 2008; 22: 1289–1296.
3. Choudhary MI, Batool I, Shah SAA, Khan SN, Atta-Ur-Rahman. Microbial Hydroxylation of oleonilic acid. Nat Prod Res. 2008; 22: 489-494.
4. Choudhary MI, Shah SAA, Musharraf SG, Shaheen F, Atta-ur-Rahman. Microbial Transformation of Dehydroepiandrosterone. Nat Prod Res. 2003; 17: 215-220.
5. Choudhary MI, Shah SAA, Sami A, Ajaz A, Shaheen F, Atta-ur-Rahman. Microbial Transformation of *E*-Guggulsterone and their Antibacterial and Antioxidant Activities. Chem Biodiv. 2005; 2: 516-524.
6. Choudhary MI, Batool I, Shah SAA, Nawaz SA, Atta-ur-Rahman. Microbial Hydroxylation of Pregnenolone Derivative and Cholinesterase Inhibitory Activity. Chem Pharma Bull. 2005; 53: 1455-1459.
7. Choudhary MI, Yousuf S, Samreen, Shah SAA, Ahmed S, Atta-ur-Rahman. Biotransformation of Physalin H and Antileishmanial Activity of Transformed Product. Chem Pharma Bull. 2006; 54: 927-930.
8. Atta-ur-Rahman, Choudhary MI, Basha FZ, Abbas G, Khan SN, Shah SAA. Science at the interface of chemistry and biology: Discoveries of α-glucosidase inhibitors and antiglycation agents. Pure Appl Chem. 2007; 79: 2263-2268.
9. Choudhary MI, Musharraf SG, Khan MTH, Abdelrahman D, Parvaz M, Shaheen F and Atta-ur-Rahman. Microbial transformation of isolongi- folen-4-one. Helv Chim Acta. 2003; 86: 3450-3460.
10. Choudhary MI, Siddiqui ZA, Nawaz SA, Atta-ur-Rahman. Microbial transformation of 18β-glycyrrhetinic acid by Cunninghamella elegans and Fusarium lini, and lipoxygenase inhibitory activity of transformed products. Nat Prod Res. 2009; 23: 507–513.
11. Demyttenaere JCR, Belleghem KV, De kimpe N. Biotransformation of (R)-(+)- and (S)-(-)-limonene by fungi and the use of solid phase microextraction for screening. Phytochemistry. 2001; 57: 199-208.
12. Fan W, Tezuka Y, Komatsu K, Namba T, Kadota S. Prolyl Endopeptidase Inhibitors from the Underground Part of Rhodiola sacra S. H. Fu. Biological & Pharmaceutical Bulletin. 1999; 22: 157-161.
13. Lee HJ, Rhee IK, Lee KB, Yoo ID, Song KS. Kynapcin-12, a New p-Terphenyl Derivative from Polyozellus multiplex, Inhibits Prolyl Endopeptidase. The Journal of Antibiotics. 2000; 53: 714-719.
14. Atta-ur-Rahman, Zareen S, Choudhary MI, Ngounou FN, Yasin A, Parvez M. Terminalin A, a novel triterpenoid from Terminalia glaucescens**.** Tetrahedron Letters. 2002; 43: 6233-6236.
15. Mahato SB, Mukherjee A. Steroid transformations by microorganisms. Phytochemistry. 1984; 23; 2131–2154.
16. Mahato SB, Banerjee S. Steroid transformations by microorganisms-II. Phytochemistry. 1985; 24: 1403–1421.
17. Mahato SB, Banerjee S, Podder S. Steroid transformations by microorganisms-III. Phytochemistry. 1989; 28: 7–40.
18. Ahmad S, Garg SK, Johri BN. Biotransformation of sterols: Selective cleavage of the side chain. Biotechnology Advances. 1992; 10: 1–67.
19. Choudhary MI, Shah SAA, Atta-ur-Rahman, Khan SN, Khan MTH. Alpha-glucosidase and tyrosinase inhibitors from fungal hydroxylation of tibolone and hydroxytibolones. Steroids. 2010; 75: 956-966.